JACS
JOURNAL OF THE AMERICAN CHEMICAL SOCIETY
pubs.acs.org/JACS
Communication

Nanosecond Metal-to-Ligand Charge-Transfer State in an Fe(II) Chromophore: Lifetime Enhancement via Nested Potentials

Justin T. Malme,[#] Reese A. Clendening,[#] Ryan Ash, Taylor Curry, Tong Ren,[*] and Josh Vura-Weis[*]

Cite This: *J. Am. Chem. Soc.* 2023, 145, 6029–6034
Read Online
ACCESS | Metrics & More | Article Recommendations | Supporting Information

ABSTRACT: Examples of Fe complexes with long-lived (≥1 ns) charge-transfer states are limited to pseudo-octahedral geometries with strong σ-donor chelates. Alternative strategies based on varying both coordination motifs and ligand donicity are highly desirable. Reported herein is an air-stable, tetragonal Fe^{II} complex, $Fe(HMTI)(CN)_2$ (HMTI = 5,5,7,12,12,14-hexamethyl-1,4,8,11-tetraazacyclotetradeca-1,3,8,10-tetraene), with a 1.25 ns metal-to-ligand charge-transfer (MLCT) lifetime. The structure has been determined, and the photophysical properties have been examined in a variety of solvents. The HMTI ligand is highly π-acidic due to low-lying π^*(C=N), which enhances Δ_{Fe} via stabilizing t_{2g} orbitals. The inflexible geometry of the macrocycle results in short Fe−N bonds, and density functional theory calculations show that this rigidity results in an unusual set of nested potential energy surfaces. Moreover, the lifetime and energy of the MLCT state depends strongly on the solvent environment. This dependence is caused by modulation of the axial ligand-field strength by Lewis acid−base interactions between the solvent and the cyano ligands. This work represents the first example of a long-lived charge transfer state in an Fe^{II} macrocyclic species.

In recent years, an intense interest has arisen in the development of chromophores based on 3d metals,[1−3] which may replace the established chromophores based on Ru or Ir in applications such as dye-sensitized solar cells[4] and photoredox catalysis.[5] Among 3d metals being studied, iron complexes are most investigated and frequently compared with their group 8 congeners (i.e., Ru).[6] In the case of Ru^{II}-based chromophores, the large ligand field splitting (Δ_{Ru}) stabilizes the triplet metal-to-ligand charge-transfer state (^{3}MLCT) compared to the metal-centered excited states (^{3,5}MC) and hence extends the ^{3}MLCT lifetime. Analogous ligand field splittings in iron complexes (Δ_{Fe}) are much smaller, promoting rapid deactivation of ^{3}MLCT via ^{3,5}MC.

The common approaches to increasing Δ_{Fe} focus on the modification of classical chelating bipyridine and terpyridine motifs, increasing σ-donicity (via C-metalation, carbene or amido moieties), enhancing π-acidity, or intensifying both σ-donicity and π-acidity using mesoionic carbenes.[6,7] Notable successes include Fe^{II} complexes with MLCT-type lifetimes of 0.528 ns (**A**, Figure 1),[8] 3 ns (**B**),[9,10] or 1 ns (**C**)[11] and Fe^{III} species with ligand-to-metal charge-transfer (LMCT) lifetimes up to 2.0 ns.[12] Coordination geometries of Fe complexes with long-lived charge-transfer states are limited to pseudo-octahedral based on tris-bidentate, bis-tridentate, and tridentate scorpionate chelate motifs.

A complementary approach toward enhancing the lifetime involves heteroleptic or "modular" complexes,[13−16] in which bidentate or tridentate chelates (which act as the charge acceptors for MLCT) are combined with some other ligands. The lifetimes of the resulting complexes have shown improvement over simple symmetric analogs (e.g., Figure 1, **D**),[14,15,17] but have been generally limited to ca. 10 ps. While the utility of these approaches has been amply demonstrated, it is desirable to expand the library of available coordination

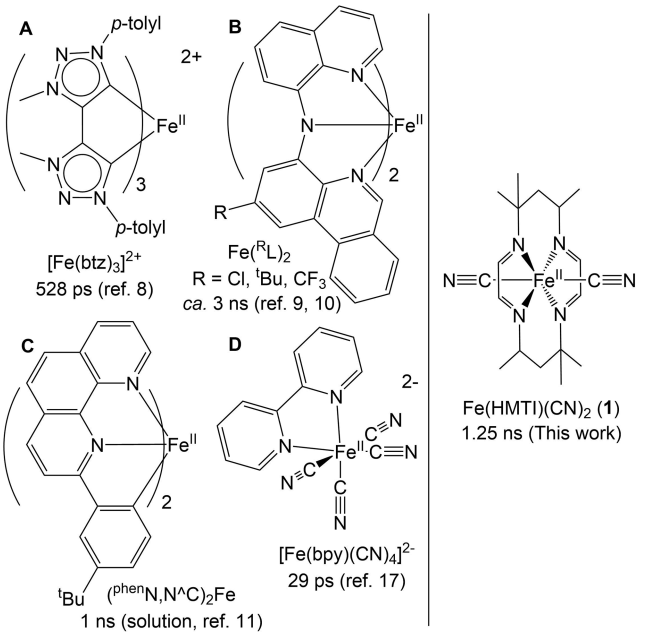

Figure 1. Illustration of selected Fe^{II} chromophores (left) and **1** (right).

Received: December 19, 2022
Published: March 13, 2023

https://doi.org/10.1021/jacs.2c13532
J. Am. Chem. Soc. 2023, 145, 6029−6034

motifs for Fe chromophores. Reported in this contribution is a demonstration of the enhancement of Δ_{Fe} within a *tetragonal* motif using a π-acidic tetradentate macrocycle, which leads to an Fe^{II} species possessing a remarkably long-lived MLCT state.

During the process of investigating the chemistry of Fe^{III}(HMC) alkynyls (HMC = 5,5,7,12,12,14-hexamethyl-1,4,8,11-tetraazacyclotetradecane), we rediscovered the conversion of Fe(HMC) compounds to Fe(HMTI) species (HMTI = 5,5,7,12,12,14-hexamethyl-1,4,8,11-tetraazacyclotetradeca-1,3,8,10-tetraene) via aerobic dehydrogenation of the HMC ring,[18] a process previously described by Busch and coworkers.[19,20] Inspired by the possibilities of a tetragonally distorted ligand field, we examined the physical attributes of cyano adduct Fe^{II}(HMTI)$(CN)_2$ (**1**; Figure 1) (see Supporting Information [SI] for synthetic details). The structure of **1** was determined via X-ray diffraction (Figure S1), confirming the two α-diimine units within the macrocycle bound to the metal center. This results in short Fe−N bonds (1.918(2)−1.939(2) Å) compared to most similar polypyridyl-based complexes (Table S1)[16,21−24] and a planar Fe-macrocycle core, with the N═C−C═N dihedral of <1°. The cyano ligands are oriented *trans* to one another, with an elongated Fe−C bond (1.955(3) Å).[22] More striking is the intense band in the absorption spectra centered at 647 nm (dichloromethane; ε = 8000 M^{-1} cm^{-1}), which is ascribed to MLCT from Fe dπ to π^*(α-diimine) (Figure S3).[20] Therefore, femtosecond UV/visible transient absorption spectroscopy was used to probe the dynamics of the state formed via excitation of this band.

Figure 2 shows selected transient spectra in $CHCl_3$ after excitation at 636 nm, with kinetic traces at 535 and 605 nm

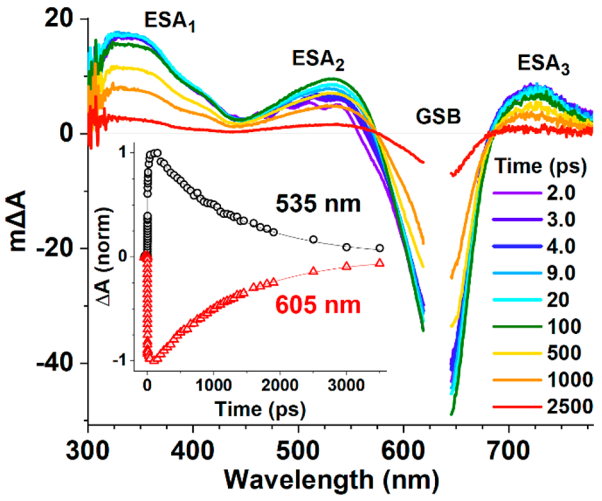

Figure 2. Transient absorption difference spectra at multiple time delays of Fe(HMTI)$(CN)_2$ in $CHCl_3$. Inset shows kinetics traces. Pump scatter (619−645 nm) has been removed.

shown in the inset. Similar spectral features are observed across various solvents (given in the SI), though as discussed below the lifetimes differ significantly. A prominent ground-state bleach (GSB) is centered around 590−640 nm in all solvents, with an excited-state absorption (ESA_2) directly to the blue, centered around 505−530 nm. This band consists of excitations of mixed cyanide−tetraimine ligand-to-metal charge-transfer character, as assigned in Figures S9 and S10. Another ESA (ESA_1) can be seen in the near-UV from a mix of π−π^* and LMCT transitions, and a third ESA is observed directly to the red of the GSB in the near-IR (ESA_3) due to low-lying LMCT excitations. These features sharpen slightly in the first 20 ps due to vibrational relaxation, then decay with an exponential time constant of 1.25 ± 0.04 ns.

This nanosecond excited state is assigned as an MLCT state on the basis of spectroelectrochemistry and density functional theory calculations. Fe(HMTI)$(CN)_2$ has a reversible $Fe^{III/II}$ oxidation at 0.14 V (versus the ferrocene couple) and an irreversible ligand-centered reduction at −1.84 V. The oxidation is significantly more anodic than typical Fe^{II} chromophores with nanosecond lifetimes (−0.61 to −0.88 V),[9−11] indicating a very electron-poor metal center in the case of **1**. As a result, **1** is exceptionally air stable (see SI). A simulated transient absorption spectrum generated from the spectra of the electrochemically oxidized/reduced complex is an excellent match with the observed transient absorption spectrum,[25] indicating that the long-lived state is of MLCT character ((spectro)electrochemical section of the SI).

Density functional theory calculations were performed in the Gaussian 16[26] and ORCA 4.2.1[27] packages at the M06L/6-311g(d) level of theory[28−31] using a polarizable continuum solvent model[32] for CH_2Cl_2. The geometries of the possible singlet, triplet, and quintet spin states were optimized (see SI for details). To understand the nanosecond lifetime, we mapped the excited-state potentials using time-dependent density functional theory (TD-DFT). A vibrational mode calculated at 347.4 cm^{-1} was selected to model the potential energy surfaces, as it had both large symmetric Fe−C displacement and symmetric Fe−N displacement in the form of expansion along a single N−Fe−N axis. These symmetric M−L displacements frequently correspond with occupation of e_g* orbitals in metal-centered states. Eight geometries were generated by vectorizing this vibrational mode and adding or subtracting multiples of the vector to the singlet ground-state geometry. Singlet and triplet single-point energies at each geometry were calculated along with a TD-DFT calculation of 50 singlets and 50 triplets.

The results of these calculations are shown in Figure 3, mapped onto the Fe−C stretch coordinate. Each excited state

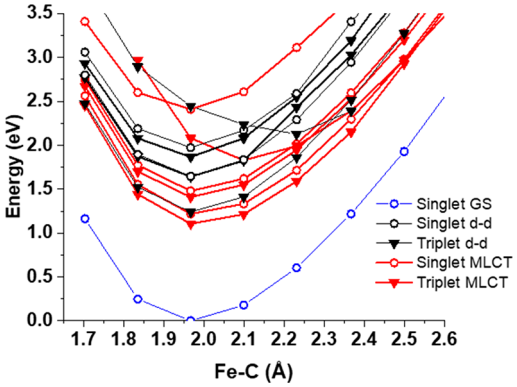

Figure 3. Manifold of states calculated at the M06L/6-311g(d) level of theory, with some higher-energy states omitted for clarity. Fe−C displacements are shown.

was designated as d−d or MLCT based on analysis of the initial and final orbitals of the highest-contributing transition, as discussed in the computational methods section of the SI. A ^{3}MLCT state is calculated to be the lowest excited state, with ^{1}MLCT and ^{3}MC states 0.113 and 0.135 eV higher in energy,

https://doi.org/10.1021/jacs.2c13532
J. Am. Chem. Soc. 2023, 145, 6029−6034

respectively. The lowest ^{5}MC is strongly distorted (Table S6) and lies ca. 0.4 eV above the lowest ^{3}MLCT (Figure S13). Along both the Fe−C and Fe−N coordinates, the potentials are well-nested, with the exception of some higher-energy triplet states.

Interestingly, the potential energy surfaces are steeper along the Fe−N than the Fe−C coordinate. An expansion/contraction of the Fe−N bonds by ca. 0.05 Å (Figure S13) results in an increase in energy of ≥1.5 eV. A similar change along the Fe−C bonds only increases the energy by ca. 0.25 eV. The dependence of the energy on the Fe−N geometry is likely a result of the macrocyclic nature of the complex and agrees well with the somewhat short Fe−N bonds observed crystallographically (*vide supra*).

This constraint may explain why the maximum MLCT lifetime of **1** (>1 ns) far exceeds those of related species such as $[Fe^{II}(bpy)(CN)_4]^{2-}$ (29 ps).[17] The macrocycle inhibits the expansion of the Fe−N bonds frequently associated with metal-centered states,[15,37] whereas such expansion with a typical bipyridine chelate is facile.[33] Intersystem crossing (ISC) is therefore rapid in the latter case due to thermally accessible curve crossings into low-energy metal-centered states. In the present case, the strong ligand field raises the metal-centered states above the lowest-energy ^{3}MLCT state, and none of the excited states intersect the ground-state surface. The small displacement between the ground- and excited-state potential energy surfaces also minimizes the vibrational wave function overlap responsible for nonradiative relaxation. This effect has been previously observed in the inherently nested spin-flip states of Cr(III) complexes or sterically restricted Cu(I) complexes.[34−36] Finally, a close inspection of Figure 3 shows that two triplet surfaces (one d−d and one MLCT) do exhibit slightly expanded Fe−C bonds; these states likely contribute to the initial fast relaxation through the excited-state manifold before the system is trapped in the lowest ^{3}MLCT state.

As shown in Figure 4, the lifetime of the MLCT excited state depends on the solvent. Moreover, **1** was found to be quite

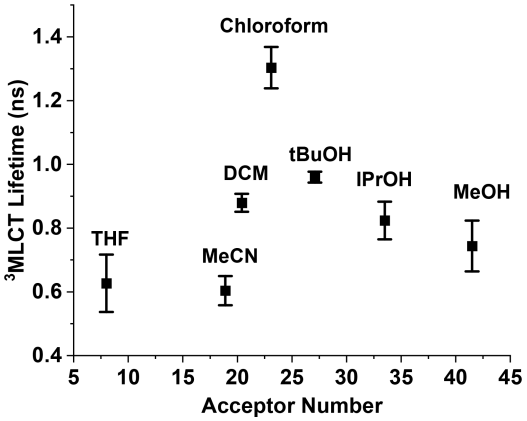

Figure 4. Acceptor number vs lifetime of the longest-lived MLCT state as observed by OTA.

solvatochromic, with the energy of the MLCT band (E_{MLCT}) varying from 1.88 eV (658 nm) in THF up to 2.07 eV (598 nm) in water. Further investigation revealed that this variation exhibited a linear dependence on the Lewis acidity of the solvent (as quantified by the acceptor number,[38] AN; Figure S25). This variation of E_{MLCT} is well documented for charge-transfer states in chromophores bearing cyano ligands[13,16,17,39,40] and likely results from Lewis acid−base interactions between the solvent and the basic nitrogen of the bound cyanide, as recently described computationally for $[Fe(bpy)(CN)_4]^{2-}$ in explicitly modeled H_2O.[41] Plots of the excited-state lifetime versus other solvent parameters such as dipole moment, dielectric constant, and viscosity did not reveal any clear trends (Figure S26).

In terms of the ligand field, the Lewis acid interaction with the nitrogen terminus diminishes the σ/π-donor character of CN^-, while enhancing its π-accepting nature.[42−44] (This may be viewed as an intermolecular extension of covalent Lewis acid-cyano adducts which have been recently investigated.[45−47]) The energies of the filled dπ and the empty d_{z^2} should therefore drop in acidic environments. The energy of the tetraimine π system is expected to stay relatively constant in contrast,[43] so E_{MLCT} concomitantly increases (Chart 1), as observed experimentally. This phenomenon allows for the influence of the axial ligand on lifetime to be evaluated.

Chart 1. Illustration of Proposed Changes in Orbital Energies as a Function of Lewis Acidity

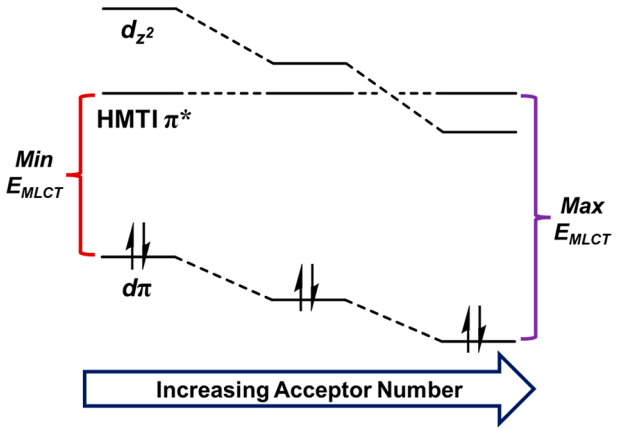

Indeed, the lifetimes vary from 627 and 604 ps (THF, AN = 8, and CH_3CN, AN = 18.9), to 1.25 ns ($CHCl_3$, AN = 23.1), to 744 ps (MeOH, AN = 41.5). A biphasic pattern emerges in which the lifetime reaches a maximum in environments of intermediate acidity. This has been previously observed for Ru(II)[39] and Fe(II)[17] species bearing cyano ligands, where the phenomenon was attributed to competing deactivation pathways. In solvents of high acceptor number (and therefore higher E_{MLCT}), the metal-centered states may become relatively lower in energy, leading to more rapid deactivation.[47] As E_{MLCT} decreases (with lower AN), deactivation via MC states becomes less significant, but direct deactivation to the ground state increases in accordance with the energy gap law. High-level *ab initio* methods including explicit solvent, combined with quantum dynamics calculations, will be needed to confirm this mechanistic hypothesis.[41]

In summary, **1** is distinct from mixed polypyridyl/cyano iron(II) chromophores in that the maximum lifetime achieved is 1.25 ns in $CHCl_3$, comparable to the MLCT states of state-of-the-art Fe^{II} chromophores (e.g., Figure 1, **A**−**C**).[9−11] In contrast, the longest MLCT lifetime achieved within a polypyridyl/cyano framework is 67 ps.[17] This nearly 20-fold leap in the lifetime of **1** versus its nearest analogues upon transition to the macrocyclic HMTI appears due—in part—to the inflexible Fe−N bonds. This results in nested potential

https://doi.org/10.1021/jacs.2c13532
J. Am. Chem. Soc. 2023, 145, 6029−6034

energy surfaces, in contrast to typical chelating motifs,[12,15] including $[Fe(bpy)(CN)_4]^{2-}$.[37] The range of lifetimes in various solvents suggests that tuning the donor/acceptor character of the axial ligand should be an effective means of altering the charge-transfer lifetime while maintaining the nested potential surfaces. Furthermore, the nature of π^*(C=N) in Fe(II) tetraimine macrocycles can be readily modified through either the change of double-bond locations or the increase in ring unsaturation, which may have a profound impact on both the energy and lifetime of the ^{3}MLCT state. This work suggests that this tetraimine, macrocyclic motif and the nested potentials it creates represent a hitherto underexplored strategy toward the development of earth-abundant alternatives to traditional 4d/5d chromophores.

■ ASSOCIATED CONTENT

Supporting Information

The Supporting Information is available free of charge at https://pubs.acs.org/doi/10.1021/jacs.2c13532.

Synthetic details; TDDFT simulated spectra and molecular orbitals; UV−vis, IR, ^{1}H NMR, and spectroelectrochemical spectra; ultrafast TA spectra and kinetic fit details; and geometries used in computational work (PDF)

Accession Codes

CCDC 2229352 contains the supplementary crystallographic data for this paper. These data can be obtained free of charge via www.ccdc.cam.ac.uk/data_request/cif, or by emailing data_request@ccdc.cam.ac.uk, or by contacting The Cambridge Crystallographic Data Centre, 12 Union Road, Cambridge CB2 1EZ, UK; fax: +44 1223 336033.

■ AUTHOR INFORMATION

Corresponding Authors

Tong Ren − *Department of Chemistry, Purdue University, West Lafayette, Indiana 47907, United States;* orcid.org/0000-0002-1148-0746; Email: tren@purdue.edu

Josh Vura-Weis − *Department of Chemistry and Materials Research Laboratory, University of Illinois at Urbana−Champaign, Urbana, Illinois 61801, United States;* orcid.org/0000-0001-7734-3130; Email: vuraweis@illinois.edu

Authors

Justin T. Malme − *Department of Chemistry, University of Illinois at Urbana−Champaign, Urbana, Illinois 61801, United States*

Reese A. Clendening − *Department of Chemistry, Purdue University, West Lafayette, Indiana 47907, United States*

Ryan Ash − *Department of Chemistry, University of Illinois at Urbana−Champaign, Urbana, Illinois 61801, United States*

Taylor Curry − *Department of Chemistry, University of Illinois at Urbana−Champaign, Urbana, Illinois 61801, United States*

Complete contact information is available at: https://pubs.acs.org/10.1021/jacs.2c13532

Author Contributions

#J.T.M. and R.A.C. contributed equally.

Notes

The authors declare no competing financial interest.

■ ACKNOWLEDGMENTS

This material is based upon work supported by the National Science Foundation under Grant Nos. 2102049 to T.R. and 2102376 to J.V.W. R.A.C. thanks Dr. Matthias Zeller for the data collection of the structure of **1**. We thank Professor James McCusker for insightful suggestions regarding acceptor number correlations. Experimental work was partially performed at the Materials Research Laboratory at the University of Illinois at Urbana−Champaign.

■ REFERENCES

(1) Wenger, O. S. Photoactive Complexes with Earth-Abundant Metals. *J. Am. Chem. Soc.* **2018**, *140*, 13522−13533.

(2) Forster, C.; Heinze, K. Photophysics and photochemistry with Earth-abundant metals - fundamentals and concepts. *Chem. Soc. Rev.* **2020**, *49*, 1057−1070.

(3) McCusker, J. K. Electronic structure in the transition metal block and its implications for light harvesting. *Science* **2019**, *363*, 484−488.

(4) Gratzel, M. Dye-sensitized solar cells. *J. Photochem. Photobiol. C* **2003**, *4*, 145−153.

(5) Chan, A. Y.; Perry, I. B.; Bissonnette, N. B.; Buksh, B. F.; Edwards, G. A.; Frye, L. I.; Garry, O. L.; Lavagnino, M. N.; Li, B. X.; Liang, Y.; Mao, E.; Millet, A.; Oakley, J. V.; Reed, N. L.; Sakai, H. A.; Seath, C. P.; MacMillan, D. W. C. Metallaphotoredox: The Merger of Photoredox and Transition Metal Catalysis. *Chem. Rev.* **2022**, *122*, 1485−1542.

(6) Wenger, O. S. Is Iron the New Ruthenium? *Chem.—Eur. J.* **2019**, *25*, 6043−6052.

(7) Dierks, P.; Vukadinovic, Y.; Bauer, M. Photoactive iron complexes: more sustainable, but still a challenge. *Inorg. Chem. Front.* **2022**, *9*, 206−220.

(8) Chabera, P.; Kjaer, K. S.; Prakash, O.; Honarfar, A.; Liu, Y. Z.; Fredin, L. A.; Harlang, T. C. B.; Lidin, S.; Uhlig, J.; Sundstrom, V.; Lomoth, R.; Persson, P.; Warnmark, K. Fe-II Hexa N-Heterocyclic Carbene Complex with a 528 ps Metal-to-Ligand Charge-Transfer Excited-State Lifetime. *J. Phys. Chem. Lett.* **2018**, *9*, 459−463.

(9) Larsen, C. B.; Braun, J. D.; Lozada, I. B.; Kunnus, K.; Biasin, E.; Kolodziej, C.; Burda, C.; Cordones, A. A.; Gaffney, K. J.; Herbert, D. E. Reduction of Electron Repulsion in Highly Covalent Fe-Amido Complexes Counteracts the Impact of a Weak Ligand Field on Excited-State Ordering. *J. Am. Chem. Soc.* **2021**, *143*, 20645−20656.

(10) Braun, J. D.; Lozada, I. B.; Kolodziej, C.; Burda, C.; Newman, K. M. E.; van Lierop, J.; Davis, R. L.; Herbert, D. E. Iron(II) coordination complexes with panchromatic absorption and nanosecond charge-transfer excited state lifetimes. *Nature Chem.* **2019**, *11*, 1144−1150.

(11) Leis, W.; Arguello Cordero, M. A.; Lochbrunner, S.; Schubert, H.; Berkefeld, A. A Photoreactive Iron(II) Complex Luminophore. *J. Am. Chem. Soc.* **2022**, *144*, 1169−1173.

(12) Kjær, K. S.; Kaul, N.; Prakash, O.; Chábera, P.; Rosemann, N. W.; Honarfar, A.; Gordivska, O.; Fredin, L. A.; Bergquist, K.-E.; Häggström, L.; Ericsson, T.; Lindh, L.; Yartsev, A.; Styring, S.; Huang, P.; Uhlig, J.; Bendix, J.; Strand, D.; Sundström, V.; Persson, P.; Lomoth, R.; Wärnmark, K. Luminescence and reactivity of a charge-transfer excited iron complex with nanosecond lifetime. *Science* **2019**, *363*, 249−253.

(13) Winkler, J. R.; Creutz, C.; Sutin, N. Solvent Tuning of the Excited-State Properties of (2,2'-Bipyridine)tetracyanoferrate(II): Direct Observation of a Metal-to-Ligand Charge-Transfer Excited State of Iron(II). *J. Am. Chem. Soc.* **1987**, *109*, 3470−3471.

(14) Paulus, B. C.; Nielsen, K. C.; Tichnell, C. R.; Carey, M. C.; McCusker, J. K. A Modular Approach to Light Capture and Synthetic Tuning of the Excited-State Properties of Fe(II)-Based Chromophores. *J. Am. Chem. Soc.* **2021**, *143*, 8086−8098.

(15) Liu, Y. Z.; Kjaer, K. S.; Fredin, L. A.; Chabera, P.; Harlang, T.; Canton, S. E.; Lidin, S.; Zhang, J. X.; Lomoth, R.; Bergquist, K. E.; Persson, P.; Warnmark, K.; Sundstrom, V. A Heteroleptic Ferrous

Complex with Mesoionic Bis(1,2,3-triazol-5-ylidene) Ligands: Taming the MLCT Excited State of Iron(II). *Chem.—Eur. J.* **2015**, *21*, 3628−3639.
(16) Vittardi, S. B.; Magar, R. T.; Schrage, B. R.; Ziegler, C. J.; Jakubikova, E.; Rack, J. J. Evidence for a lowest energy 3MLCT excited state in [Fe(tpy)(CN)3]-. *Chem. Commun.* **2021**, *57*, 4658−4661.
(17) Kunnus, K.; Li, L.; Titus, C. J.; Lee, S. J.; Reinhard, M. E.; Koroidov, S.; Kjaer, K. S.; Hong, K.; Ledbetter, K.; Doriese, W. B.; O'Neil, G. C.; Swetz, D. S.; Ullom, J. N.; Li, D.; Irwin, K.; Nordlund, D.; Cordones, A. A.; Gaffney, K. J. Chemical control of competing electron transfer pathways in iron tetracyano-polypyridyl photosensitizers. *Chem. Sci.* **2020**, *11*, 4360−4373.
(18) Clendening, R. A.; Ren, T. Mono- and Bis-alkynyl Iron Complexes Supported by a ″Softened″ Tetraaza Macrocycle. *Eur. J. Inorg. Chem.* **2022**, *2022*, No. e202101021.
(19) Dabrowiak, J. C.; Lovecchio, F. V.; Goedken, V. L.; Busch, D. H. Synthesis and electrochemical behavior of a new series of macrocyclic complexes of iron produced by oxidative dehydrogenation and tautomerization. *J. Am. Chem. Soc.* **1972**, *94*, 5502−5504.
(20) Dabrowiak, J. C.; Busch, D. H. Iron complexes with macrocyclic ligands containing the.alpha.-diimine functional unit and its position-specific formation under the influence of the iron atom. *Inorg. Chem.* **1975**, *14*, 1881−1888.
(21) Lu, T.-H.; Kao, H.-Y.; Wu, D. I.; Kong, K. C.; Cheng, C. H. Structure of Bis(2,2'-bipyridine)dicyanoiron(III) Perchlorate. *Acta Cryst. C* **1988**, *44*, 1184−1186.
(22) Nieuwenhuyzen, M.; Bertram, B.; Gallagher, J. F.; Vos, J. G. Dipotassium (2,2'-Bipyridyl-*N*,*N*')-tetracyanoferrate(II) 2.5-Hydrate, $K_2[Fe(bpy)(CN)_4].2.5H_2O$. *Acta Cryst. C* **1998**, *54*, 603−606.
(23) Zhan, S.; Meng, Q.; You, X.; Wang, G.; Zheng, P.-J. The Properties, Crystal and Molecular Structure of *Cis*-Dicyano-Bis(1,10-Phenanthroline)Iron(II) Trihydrate. *Polyhedron* **1996**, *15*, 2655−2658.
(24) Wang, Y.; Ma, X.; Hu, S.; Wen, Y.; Xue, Z.; Zhu, X.; Zhang, X.; Sheng, T.; Wu, X. Syntheses, crystal structures, MMCT and magnetic properties of four one-dimensional cyanide-bridged complexes comprised of MII-CN-FeIII (M = Fe, Ru, Os). *Dalton Trans* **2014**, *43*, 17453−17462.
(25) Brown, A. M.; McCusker, C. E.; McCusker, J. K. Spectroelectrochemical identification of charge-transfer excited states in transition metal-based polypyridyl complexes. *Dalton Trans* **2014**, *43*, 17635−17646.
(26) Frisch, M. J.; Trucks, G. W.; Schlegel, H. B.; Scuseria, G. E.; Robb, M. A.; Cheeseman, J. R.; Scalmani, G.; Barone, V.; Petersson, G. A.; Nakatsuji, H.; Li, X.; Caricato, M.; Marenich, A. V.; Bloino, J.; Janesko, B. G.; Gomperts, R.; Mennucci, B.; Hratchian, H. P.; Ortiz, J. V.; Izmaylov, A. F.; Sonnenberg, J. L.; Williams-Young, D.; Ding, F.; Lipparini, F.; Egidi, F.; Goings, J.; Peng, B.; Petrone, A.; Henderson, T.; Ranasinghe, D.; Zakrzewski, V. G.; Gao, J.; Rega, N.; Zheng, G.; Liang, W.; Hada, M.; Ehara, M.; Toyota, K.; Fukuda, R.; Hasegawa, J.; Ishida, M.; Nakajima, T.; Honda, Y.; Kitao, O.; Nakai, H.; Vreven, T.; Throssell, K.; Montgomery, J. A., Jr.; Peralta, J. E.; Ogliaro, F.; Bearpark, M. J.; Heyd, J. J.; Brothers, E. N.; Kudin, K. N.; Staroverov, V. N.; Keith, T. A.; Kobayashi, R.; Normand, J.; Raghavachari, K.; Rendell, A. P.; Burant, J. C.; Iyengar, S. S.; Tomasi, J.; Cossi, M.; Millam, J. M.; Klene, M.; Adamo, C.; Cammi, R.; Ochterski, J. W.; Martin, R. L.; Morokuma, K.; Farkas, O.; Foresman, J. B.; Fox, D. J. *Gaussian 16 Rev. A.03*; Wallingford, CT, 2016.
(27) Neese, F.; Wennmohs, F.; Becker, U.; Riplinger, C. The ORCA quantum chemistry program package. *J. Chem. Phys.* **2020**, *152*, 224108.
(28) Becke, A. D. Density-functional thermochemistry. III. The role of exact exchange. *J. Chem. Phys.* **1993**, *98*, 5648−5652.
(29) Raghavachari, K.; Trucks, G. W. Highly correlated systems: Excitation energies of first row transition metals Sc-Cu. *J. Chem. Phys.* **1989**, *91*, 1062−1065.
(30) Hay, P. J. Gaussian basis sets for molecular calculations − representation of 3D orbitals in transition-metal atoms. *J. Chem. Phys.* **1977**, *66*, 4377−4384.
(31) Wachters, A. J. H. Gaussian basis set for molecular wavefunctions containing third-row atoms. *J. Chem. Phys.* **1970**, *52*, 1033.
(32) Cossi, M.; Rega, N.; Scalmani, G.; Barone, V. Energies, structures, and electronic properties of molecules in solution with the C-PCM solvation model. *J. Comput. Chem.* **2003**, *24*, 669−681.
(33) Kjaer, K. S.; Van Driel, T. B.; Harlang, T. C. B.; Kunnus, K.; Biasin, E.; Ledbetter, K.; Hartsock, R. W.; Reinhard, M. E.; Koroidov, S.; Li, L.; Laursen, M. G.; Hansen, F. B.; Vester, P.; Christensen, M.; Haldrup, K.; Nielsen, M. M.; Dohn, A. O.; Papai, M. I.; Moller, K. B.; Chabera, P.; Liu, Y. Z.; Tatsuno, H.; Timm, C.; Jarenmark, M.; Uhlig, J.; Sundstom, V.; Warnmark, K.; Persson, P.; Nemeth, Z.; Szemes, D. S.; Bajnaczi, E.; Vanko, G.; Alonso-Mori, R.; Glownia, J. M.; Nelson, S.; Sikorski, M.; Sokaras, D.; Canton, S. E.; Lemke, H. T.; Gaffney, K. J. Finding intersections between electronic excited state potential energy surfaces with simultaneous ultrafast X-ray scattering and spectroscopy. *Chem. Sci.* **2019**, *10*, 5749−5760.
(34) Otto, S.; Dorn, M.; Forster, C.; Bauer, M.; Seitz, M.; Heinze, K. Understanding and exploiting long-lived near-infrared emission of a molecular ruby. *Coord. Chem. Rev.* **2018**, *359*, 102−111.
(35) Mara, M.; Fransted, K.; Chen, L. Interplays of excited state structures and dynamics in copper(I) diimine complexes: Implications and perspectives. *Coord. Chem. Rev.* **2015**, *282*−*283*, 2−18.
(36) Forster, L. S. Thermal relaxation in excited electronic states of d(3) and d(6) metal complexes. *Coord. Chem. Rev.* **2002**, *227*, 59−92.
(37) Zhang, W. K.; Kjaer, K. S.; Alonso-Mori, R.; Bergmann, U.; Chollet, M.; Fredin, L. A.; Hadt, R. G.; Hartsock, R. W.; Harlang, T.; Kroll, T.; Kubicek, K.; Lemke, H. T.; Liang, H. W.; Liu, Y. Z.; Nielsen, M. M.; Persson, P.; Robinson, J. S.; Solomon, E. I.; Sun, Z.; Sokaras, D.; van Driel, T. B.; Weng, T. C.; Zhu, D. L.; Warnmark, K.; Sundstrom, V.; Gaffney, K. J. Manipulating charge transfer excited state relaxation and spin crossover in iron coordination complexes with ligand substitution. *Chem. Sci.* **2017**, *8*, 515−523.
(38) Mayer, U.; Gutmann, V.; Gerger, W. The Acceptor Number - A Quantitative Empirical Parameter for the Electrophilic Properties of Solvents. *Monatsh. Chem.* **1975**, *106*, 1235−1257.
(39) Indelli, M. T.; Bignozzi, C. A.; Scandola, F.; Collin, J.-P. Design of Long-Lived Ru(II) Terpyridine MLCT States. Tricyano Terpyridine Complexes. *Inorg. Chem.* **1998**, *37*, 6084−6089.
(40) Soukup, R. W.; Schmid, R. Metal Complexes as Color Indicators for Solvent Parameters. *J. Chem. Educ.* **1985**, *62*, 459−462.
(41) Zederkof, D. B.; Moller, K. B.; Nielsen, M. M.; Haldrup, K.; Gonzalez, L.; Mai, S. Resolving Femtosecond Solvent Reorganization Dynamics in an Iron Complex by Nonadiabatic Dynamics Simulations. *J. Am. Chem. Soc.* **2022**, *144*, 12861−12873.
(42) Kjaer, K. S.; Kunnus, K.; Harlang, T. C. B.; Van Driel, T. B.; Ledbetter, K.; Hartsock, R. W.; Reinhard, M. E.; Koroidov, S.; Li, L.; Laursen, M. G.; Biasin, E.; Hansen, F. B.; Vester, P.; Christensen, M.; Haldrup, K.; Nielsen, M. M.; Chabera, P.; Liu, Y. Z.; Tatsuno, H.; Timm, C.; Uhlig, J.; Sundstom, V.; Nemeth, Z.; Szemes, D. S.; Bajnoczi, E.; Vanko, G.; Alonso-Mori, R.; Glownia, J. M.; Nelson, S.; Sikorski, M.; Sokaras, D.; Lemke, H. T.; Canton, S. E.; Warnmark, K.; Persson, P.; Cordones, A. A.; Gaffney, K. J. Solvent control of charge transfer excited state relaxation pathways in Fe(2,2 '-bipyridine)(CN)(4) (2-). *Phys. Chem. Chem. Phys.* **2018**, *20*, 4238−4249.
(43) Timpson, C. J.; Bignozzi, C. A.; Sullivan, B. P.; Kober, E. M.; Meyer, T. J. Influence of Solvent on the Spectroscopic Properties of Cyano Complexes of Ruthenium(II). *J. Phys. Chem.* **1996**, *100*, 2915−2925.
(44) Jay, R. M.; Vaz da Cruz, V. c.; Eckert, S.; Fondell, M.; Mitzner, R.; Fohlisch, A. Probing Solute-Solvent Interactions of Transition Metal Complexes Using L-Edge Absorption Spectroscopy. *J. Phys. Chem. B* **2020**, *124*, 5636−5645.
(45) Ngo, D. X.; Del Ciello, S. A.; Barth, A. T.; Hadt, R. G.; Grubbs, R. H.; Gray, H. B.; McNicholas, B. J. Electronic Structures, Spectroscopy, and Electrochemistry of $[M(diimine)(CN\text{-}BR_3)_4]^{2-}$

https://doi.org/10.1021/jacs.2c13532
J. Am. Chem. Soc. 2023, 145, 6029−6034

(M = Fe, Ru; R = Ph, C_6F_5) Complexes. *Inorg. Chem.* **2020**, *59*, 9594−9604.
(46) Schmid, L.; Kerzig, C.; Prescimone, A.; Wenger, O. S. Photostable Ruthenium(II) Isocyanoborato Luminophores and Their Use in Energy Transfer and Photoredox Catalysis. *JACS Au* **2021**, *1*, 819−832.
(47) Schmid, L.; Chabera, P.; Ruter, I.; Prescimone, A.; Meyer, F.; Yartsev, A.; Persson, P.; Wenger, O. S. Borylation in the Second Coordination Sphere of FeII Cyanido Complexes and Its Impact on Their Electronic Structures and Excited-State Dynamics. *Inorg. Chem.* **2022**, *61*, 15853−15863.

https://doi.org/10.1021/jacs.2c13532
J. Am. Chem. Soc. 2023, 145, 6029−6034